Reduced structural brain connectivity in amyotrophic lateral sclerosis

Colin R. Buchanan[1]
c.r.buchanan-2@sms.ed.ac.uk
Lewis D. Pettit[2]
l.d.pettit@sms.ed.ac.uk
Mark E. Bastin[3]
mark.bastin@ed.ac.uk
Amos J. Storkey[1]
a.storkey@ed.ac.uk
Sharon Abrahams[2]
s.abrahams@ed.ac.uk

[1] School of Informatics, University of Edinburgh, Edinburgh, UK
[2] School of Philosophy, Psychology and Language Sciences, University of Edinburgh, Edinburgh, UK
[3] Medical and Radiological Sciences, University of Edinburgh, Edinburgh, UK

Abstract

Magnetic resonance imaging (MRI) and network analysis was used to assess the connectivity between brain regions in a group of 30 amyotrophic lateral sclerosis (ALS) patients when compared with a group of age-matched healthy controls. For each subject, 85 grey matter regions (network nodes) were identified from high resolution structural MRI and network connections were formed from the white matter tracts generated by diffusion MRI and probabilistic tractography. Whole-brain networks were constructed using an anatomically motivated white matter waypoint constraint and a weighting reflecting tract-averaged fractional anisotropy. An established statistical technique called network-based statistics was then used, without *a priori* selected regions, to identify a subnetwork (13 nodes and 13 bidirectional connections) of reduced connectivity in the ALS group compared with the controls ($p = 0.021$, corrected). These findings suggest that degeneration in ALS is strongly linked to the motor cortex.

1 Introduction

Amyotrophic lateral sclerosis (ALS), the most common form of motor neurone disease, is a devastating neurodegenerative disorder affecting upper and lower motor neurons in the motor cortex, brain stem and spinal cord [11]. Though the aetiology of ALS is not well understood, magnetic resonance imaging (MRI) has proved useful in probing the white matter degeneration attributed to ALS [1, 5]. It is possible that network analyses may improve understanding of the degeneration in connectivity. Whole-brain structural networks [13] can be constructed from MRI data, with network nodes identified from high resolution structural MRI and network connections formed by the white matter tracts generated from diffusion MRI (dMRI) and tractography. Statistical techniques, such as network-based statistics (NBS) [16], can then be used to identify impairments in connectivity due to ALS.

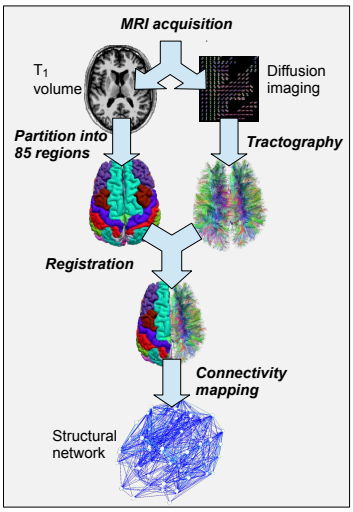

Figure 1: An overview of the processing pipeline for constructing a whole-brain network from T_1-weighted and dMRI data.

2 Materials and methods

30 ALS patients (mean age 58.3 ± 11.2 years, 17 male, ALS Function Rating Scale-revised score > 20) and 30 healthy controls (mean age 58.5 ± 12.0 years, 16 male) were recruited and underwent an MRI protocol. All imaging data were acquired using a GE Signa HDxt 1.5 T clinical scanner. For the dMRI protocol, single-shot spin-echo echo-planar (EP) diffusion-weighted whole-brain volumes ($b = 1000$ s/mm^2) were acquired in 64 non-collinear directions, along with seven T_2-weighted volumes at $2 \times 2 \times 2$ mm resolution. 3D T_1-weighted inversion-recovery prepared, fast spoiled gradient-echo volumes were acquired at $1 \times 1 \times 1.3$ mm resolution in the coronal plane.

An automated connectivity mapping pipeline was developed to construct white matter structural networks from T_1-weighted and dMRI data (Fig. 1). This framework is described below with settings informed by the findings from a test-retest study using healthy volunteers [4]. Each T_1-weighted brain was divided into distinct neuroanatomical regions using the volumetric segmentation and cortical reconstruction performed with the FreeSurfer image analysis suite using the default parameters. The Desikan-Killiany atlas delineated 34 cortical structures per hemisphere [6, 8]. Additionally, sub-cortical segmentation was applied to obtain 8 grey matter structures per hemisphere plus the brain stem [7]. As a result, 85 regions-of-interest (ROIs) were retained per subject. The results of the segmentation procedure were used to construct grey and white matter masks for each subject.

The dMRI data underwent eddy current correction to counteract systematic imaging distortions and patient motion using affine registration to the first T_2-weighted volume of each subject [9]. Fractional anisotropy (FA) was calculated at each voxel location measuring the degree of anisotropic diffusion,

$$\text{FA} = \sqrt{\frac{1}{2}} \frac{\sqrt{(\lambda_1 - \lambda_2)^2 + (\lambda_2 - \lambda_3)^2 + (\lambda_3 - \lambda_1)^2}}{\sqrt{\lambda_1^2 + \lambda_2^2 + \lambda_3^2}}, \tag{1}$$

where $(\lambda_1, \lambda_2, \lambda_3)$ are the eigenvalues of the diffusion tensor [3]. Skull stripping and brain extraction were performed on the T_2-weighted volumes and applied to the FA volume of each session [12]. A cross-modal non-linear registration protocol was used to align neuroanatomical ROIs from T_1-weighted volume to diffusion space. Firstly, linear registration [9] was used to initialise the alignment of each brain-extracted FA volume to the corresponding FreeSurfer extracted brain using a mutual information cost function and an affine transform with 12 degrees of freedom. Following this initialisation, a non-linear deformation field based method [2] was used to refine local alignment. FreeSurfer segmentations and anatomical labels were then aligned to diffusion space using nearest neighbour interpolation.

Tractography was then initiated from all voxels within each grey matter ROI using an established probabilistic tensor tractography algorithm [10]. Probability density functions (PDFs) were computed at each voxel location, which capture the uncertainty in the principal directions of diffusion. PDFs were described with a rotationally symmetric Watson distribution and estimated from the dMRI data. From each seed point 100 streamlines were constructed from voxel to voxel until terminated by stopping criteria, specifically, curvature exceeding 80 degrees, FA below 0.1, or entering an extra-cerebral voxel.

Connections were computed by recording connections between all ROI pairs. The endpoint of a streamline was considered to be the first grey matter ROI encountered when tracking from the seed location. Streamlines were only considered valid if they had passed through at least one white matter waypoint voxel. The white matter regions obtained from FreeSurfer were used as the waypoint mask. FA weighted networks were constructed where each entry in an 85×85 adjacency matrix was computed,

$$a_{ij} = \frac{1}{|S_{ij}|} \sum_{s \in S_{ij}} \frac{\sum_{v \in V_s} \mathrm{FA}(v)}{m_s}, \tag{2}$$

where S_{ij} is the set of streamlines originating from node i and terminating at node j, V_s is the set of m_s voxels found along the streamline between the seed point of streamline s and the first voxel encountered at node j. FA measures the diffusion anisotropy per voxel. As tractography cannot distinguish between afferent and efferent connections, the weights in the adjacency matrix were made symmetric across the diagonal, $\hat{a}_{ij} = \frac{1}{2}(a_{ij} + a_{ji})$, resulting in an undirected positive-weighted graph. Self-connections were removed.

Connectivity within these networks was compared between the ALS and control groups using NBS [16], without *a priori* selected regions. NBS exploits the extent to which the connections identified by the contrast are interconnected to offer a potential gain in statistical power. As tractography is known to produce some false connections [14], we examined a number of thresholded networks for which connections were only retained if they occurred in at least a certain proportion of subjects. In the NBS framework, first a two-sample t-test was performed at each of the 3570 network connections to identify differences between the ALS and control groups. Secondly, a set of suprathreshold edges and the corresponding set of maximally connected network components was computed. Finally, permutation testing with 5000 iterations was used to estimate the distribution of component size and compute a corrected p-value for the maximally connected subnetwork(s).

3 Results

Approximately 6 million streamlines were seeded per subject (Fig. 2(a)) and networks constructed as described. Two ALS sessions were discarded due to incomplete data or patient

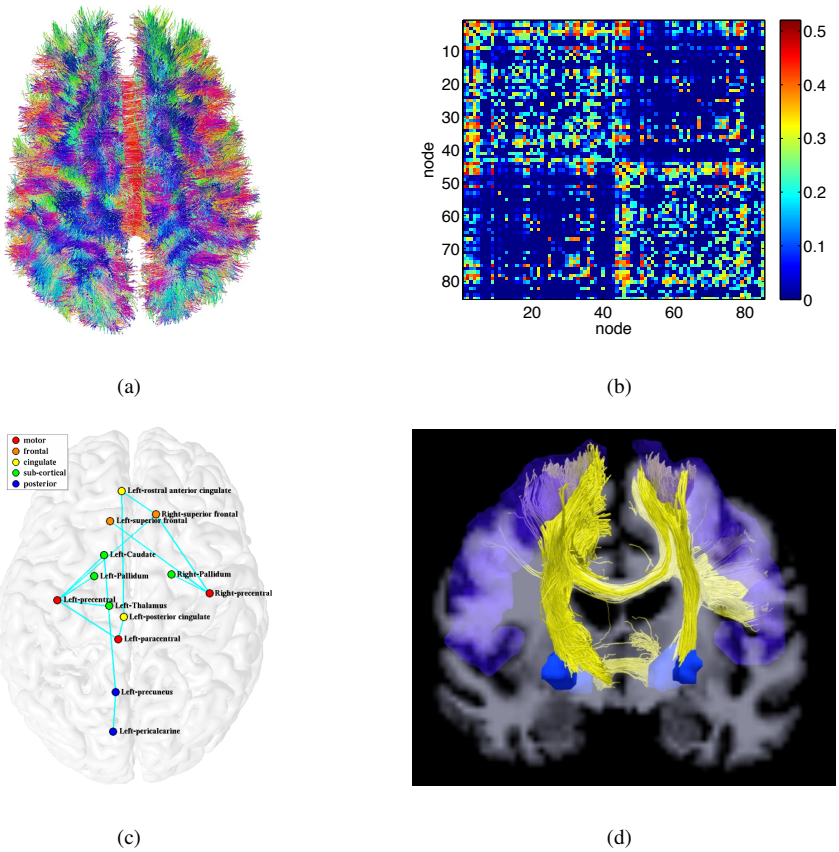

(a) (b)

(c) (d)

Figure 2: (a) Example streamlines for one subject (56 year old male); (b) 85×85 connectivity matrix showing connections averaged across all subjects, where the two large rectangular patterns on the diagonal correspond to the left and right hemispheres; (c) Network showing the nodes and interconnections identified by NBS where node location is indicated by colour; (d) Coronal view of the tracts (yellow) involved in the subnetwork identified by NBS for one subject (63 year old female) where colouring indicates the precentral gyrus and pallidum.

motion. Figure 2(b) shows the mean connectivity matrix averaged across all subjects. Findings from a one-way ANOVA suggest there is no difference in the global network 'strength' (mean of each subject's connectivity matrix) between the ALS and control groups. However, NBS identified a subnetwork (13 nodes and 13 bidirectional connections, Fig. 2(c)) of reduced connectivity in the ALS group ($p = 0.021$, corrected). The same network was produced over several different network thresholds (tested over thresholds for which connections occurred in at least 10-50% of subjects), indicating that the NBS procedure is largely robust to possible false connections. This subnetwork involves three nodes within the primary motor cortex (left and right precentral, left paracentral), bilateral superior frontal connections, four subcortical areas (left and right pallidum, left thalamus, left caudate), two nodes in the left cingulate cortex (posterior and rostral anterior) and two posterior nodes (left precuneus, left pericalcarine). Eight of the thirteen connections are to nodes within the primary motor

cortex. Figure 2(d) shows an example of the tracts involved in the subnetwork identified by NBS for one subject. On average, the connections in this subnetwork showed a 0.062 ± 0.09 reduction in tract-averaged FA in the ALS group compared with the controls, whereas no difference in global network strength was found between the two groups.

4 Conclusions

Previous dMRI studies have shown reduced white matter integrity in the cortico-spinal tract and corpus callosum [1, 5], areas which are interlinked with several of the sub-cortical and motor cortex nodes identified by our subnetwork (Fig. 2(d)). A previous NBS study [15] identified a nine node network which found a similar pattern of impairment involving connections to precentral, paracentral, pallidum, frontal areas and the cingulate cortex. Our results suggest that in ALS, connectivity to prefrontal, precentral, subcortical and some posterior regions is substantially reduced, in terms of tract-averaged FA, and that these impaired connections are predominantly localised around the motor cortex. However, the posterior connections identified are not typically associated with ALS. We note that although NBS reduces the false positive rate, tractography can still produce both false positive and false negative connections. However, as the brain is a strongly interconnected system, it is also possible that the degeneration of motor neurons may result in a distributed effect on the brain network. These findings suggest that, though changes in structural connectivity may be widespread in ALS, overall the degeneration is strongly linked to the motor cortex. It is possible that these areas of reduced connectivity may underlie some of the cognitive impairments associated with the disease.

Acknowledgements

This work was supported by a Sylvia Aitken Charitable Trust grant. CB was funded by the Engineering and Physical Sciences Research Council and the Medical Research Council through the Neuroinformatics and Computational Neuroscience Doctoral Training Centre, University of Edinburgh.

References

[1] F. Agosta, E. Pagani, M. Petrolini, D. Caputo, M. Perini, A. Prelle, F. Salvi, and M. Filippi. Assessment of white matter tract damage in patients with amyotrophic lateral sclerosis: a diffusion tensor MR imaging tractography study. *American Journal of Neuroradiology*, 31(8):1457–1461, 2010.

[2] J. L. R. Andersson, M. Jenkinson, and S. Smith. Non-linear registration aka Spatial normalisation. Technical Report TR07JA2, Oxford Centre for Functional Magnetic Resonance Imaging of the Brain, University of Oxford, June 2007.

[3] P. J. Basser and C. Pierpaoli. Microstructural and physiological features of tissues elucidated by quantitative-diffusion-tensor MRI. *Journal of magnetic resonance Series B*, 111(3):209–219, 1996.

[4] C. R. Buchanan, C. R. Pernet, K. J. Gorgolewski, A. J. Storkey, and M. E. Bastin. Test-retest reliability of structural brain networks from diffusion MRI. *"in preparation"*, 2013.

[5] M. Cirillo, F. Esposito, G. Tedeschi, G. Caiazzo, A. Sagnelli, G. Piccirillo, R. Conforti, F. Tortora, M R Monsurrò, S. Cirillo, and F. Trojsi. Widespread Microstructural White Matter Involvement in Amyotrophic Lateral Sclerosis: A Whole-Brain DTI Study. *American Journal Of Neuroradiology*, pages 1–7, 2012. ISSN 1936959X.

[6] R. S. Desikan, F. Ségonne, B. Fischl, B. T. Quinn, B. C. Dickerson, D. Blacker, R. L. Buckner, A. M. Dale, R. P. Maguire, B. T. Hyman, M. S. Albert, and R. J. Killiany. An automated labeling system for subdividing the human cerebral cortex on MRI scans into gyral based regions of interest. *NeuroImage*, 31(3):968–980, 2006.

[7] B. Fischl, D. H. Salat, E. Busa, M. Albert, M. Dieterich, C. Haselgrove, A. Van Der Kouwe, R. Killiany, D. Kennedy, S. Klaveness, A. Montillo, N. Makris, B. Rosen, and A. M. Dale. Whole Brain Segmentation: Neurotechnique Automated Labeling of Neuroanatomical Structures in the Human Brain. *Neuron*, 33(3):341–355, 2002. ISSN 08966273.

[8] B. Fischl, A. Van Der Kouwe, C. Destrieux, E. Halgren, F. Ségonne, D. H. Salat, E. Busa, L. J. Seidman, J. Goldstein, D. Kennedy, V. Caviness, N Makris, B. Rosen, and A. M. Dale. Automatically parcellating the human cerebral cortex. *Cerebral Cortex*, 14(1):11–22, 2004.

[9] M. Jenkinson and S. Smith. A global optimisation method for robust affine registration of brain images. *Medical Image Analysis*, 5(2):143–156, 2001.

[10] G. J. M. Parker, H. A. Haroon, and C. A. M. Wheeler-Kingshott. A framework for a streamline-based probabilistic index of connectivity (PICo) using a structural interpretation of MRI diffusion measurements. *Journal of Magnetic Resonance Imaging*, 18 (2):242–254, 2003.

[11] L. P. Rowland and N. A. Shneider. Amyotrophic lateral sclerosis. *New England Journal of Medicine*, 344(22):1688–1700, 2001.

[12] S. M. Smith. Fast robust automated brain extraction. *Human Brain Mapping*, 17(3): 143–155, 2002. ISSN 10659471.

[13] O. Sporns. The human connectome: a complex network. *Annals Of The New York Academy Of Sciences*, 1224(1):109–125, 2011.

[14] D. C. Van Essen and K. Ugurbil. The future of the human connectome. *NeuroImage*, 62(2):1–12, 2012. ISSN 10959572.

[15] E. Verstraete, J. H. Veldink, R. C. W. Mandl, L. H. Van Den Berg, and M. P. Van Den Heuvel. Impaired Structural Motor Connectome in Amyotrophic Lateral Sclerosis. *PLoS ONE*, 6(9):10, 2011.

[16] A. Zalesky, A. Fornito, and E. T. Bullmore. Network-based statistic: identifying differences in brain networks. *NeuroImage*, 53(4):1197–1207, 2010.